PHYSICAL REVIEW D **89,** 065013 (2014)

Clustering and decomposition for non-BPS solutions of the $\mathbb{CP}^{N-1}$ models

S. Bolognesi* and W. Zakrzewski†

Department of Mathematical Sciences, Durham University, Durham DH1 3LE, United Kingdom

(Received 14 November 2013; published 13 March 2014)

We look at solutions [both Bogomol'nyi-Prasad-Sommerfield (BPS) and non-BPS] of the $\mathbb{CP}^{N-1}$ model on $\mathbb{R} \times S^1$ (with twisted boundary conditions), in particular by using a conformal mapping technique, and we show how to interpret these solutions by decomposing them into expressions describing constituent solitons. We point out the problems that may arise (for non-BPS solutions) when one naively looks at the clustering properties of these solutions. This could lead to misunderstandings when studying extrapolations between small and large compactification radii.

DOI: 10.1103/PhysRevD.89.065013 PACS numbers: 11.10.Kk, 04.20.Jb, 11.27.+d

I. INTRODUCTION

The $\mathbb{CP}^{N-1}$ nonlinear sigma model on the Euclidean plane $\mathbb{R}^2$ has holomorphic and antiholomorphic solutions which saturate the Bogomol'nyi-Prasad-Sommerfield (BPS) bound and minimize the action in any given topological sector [1]. When $N > 2$ there are also additional solutions, which are not BPS and which are only unstable saddle points of the action. These solutions have been extensively studied in the past on the $\mathbb{R}^2$ and S^2 backgrounds [2–5]. There exists a solution generating technique which allows one to construct these non-BPS solutions from the holomorphic (or antiholomorphic) ones by acting on them, several times, with certain operators $P_{\pm}$. A number of theorems have been rigorously established, in particular the proof that this procedure is complete, in the sense that all such solutions can be obtained by the repeated action of one of these operators on the holomorphic (or antiholomorphic) solutions.

Some recent papers have revitalized the interest in non-BPS solutions of sigma models defined on Euclidean space and, in particular, also on the cylinder $\mathbb{R} \times S^1$ [6–8]. Compactification deforms the original quantum field theory (QFT) by introducing an infrared cutoff, thus bringing the theory to a region in which it becomes tractable as a semiclassical quantum mechanical system. The main goal of these approaches is to try to provide a rigorous mathematical definition of the QFT by invoking the principle of continuous connection between small and large compactification radii [9–11]. Establishing this continuous connection is probably one of the main difficult points that have to be clarified to achieve the success of this program.

Holomorphic solutions of the $\mathbb{CP}^{N-1}$ sigma model on $\mathbb{R} \times S^1$ have been studied in [12–14] and they have many properties in common with instantons on $\mathbb{R}^3 \times S^1$. In the $\mathbb{CP}^{N-1}$ the boundary conditions are parametrized by N real angles θ_I. The "strictly" periodic boundary conditions correspond to the case when all the angles are equal. When the angles are maximally separated, i.e. $\theta_I = 2\pi I/N$, we say that we have the so-called "twisted" boundary conditions. Continuity between small and large compactification radii works very well in the holomorphic sector. As the size of the compactified direction is varied, while keeping the soliton size fixed, the action and the number of zero modes around a given solution remain constant. However, the properties of the solutions do change. For example, for a generic choice of the angles θ_I, a soliton (topological charge one) may split into "partons" which carry a fraction of the topological charge.

For the twisted boundary conditions a one-soliton splits into N partons which carry $1/N$th of the topological charge and are related by a residual $\mathbb{Z}_N$ symmetry. This is a crucial effect which allows us to relate the strong-coupling effects of the original QFT defined on the plane to this modified theory in a weak-coupling regime and thus to investigate their properties in a semiclassical expansion.

The main goal of this paper is to extend these studies to a nonholomorphic case, i.e. to study in detail the nonholomorphic solutions on $\mathbb{R} \times S^1$, placing particular emphasis on trying to understand how in this case they interpolate between small and large compactification radii. In Sec. II we rephrase some known results about the compactified $\mathbb{CP}^{N-1}$ sigma model by using a conformal mapping technique and mapping from $\mathbb{R} \times S^1$ to $\mathbb{R}^2$. This approach will allow us to establish some new results on the properties of nonholomorphic solutions. In Sec. III we recall some facts about the operators $P_{\pm}$ which will be very useful in order to study the properties of the nonholomorphic solutions on $\mathbb{R} \times S^1$. Section IV discusses the behavior of such nonholomorphic solutions in the embedding and clustering limits and shows that, in many aspects, this behavior is different from the behavior of the holomorphic solutions.

II. $\mathbb{CP}^{N-1}$ SIGMA MODEL ON A PLANE AND ON A CYLINDER

The complex projective space $\mathbb{CP}^{N-1}$ model can be parametrized by a vector with N complex components

*s.bolognesi@durham.ac.uk
†w.j.zakrzewski@durham.ac.uk

$n = (n_1, \ldots, n_N)$ of unit norm $n^\dagger n = 1$ supplemented by gauging away the overall $U(1)$ phase $n \equiv e^{i\alpha} n$. The action of such a sigma model on the Euclidean plane (x_1, x_2) is

$$S = \int d^2x D_\mu n^\dagger D_\mu n, \tag{2.1}$$

where the covariant derivative is $D_\mu = \partial_\mu - iA_\mu$ and the gauge field is a composite of the field n itself and is given by $A_\mu = -in^\dagger \partial_\mu n$. The Euler-Lagrange equations for the field n are given by

$$D_\mu D_\mu n - (n^\dagger D_\mu D_\mu n) n = 0 \tag{2.2}$$

together with the constraint $n^\dagger n = 1$. The action is classically conformally invariant, so any conformal transformation maps solutions of the Euler-Lagrange equations into other solutions. We will use this property very frequently in this paper.

A cylinder can be obtained from a plane by imposing on it periodicity in one direction, say $x_1 = x_1 + L$ and we can set $L = 1$ by conformal rescaling. The $\mathbb{CP}^{N-1}$ field can be taken to be "almost" periodic, that is, periodic up to a unitary matrix transformation $\Omega \in U(N)$:

$$n(x_1 + 1, x_2) = \Omega n(x_1, x_2). \tag{2.3}$$

We can diagonalize Ω and recast it into a canonical form

$$\Omega = \mathrm{diag}(1, e^{i\theta_1}, \ldots, e^{i\theta_{N-1}}) \tag{2.4}$$

with $\theta_1 \le \cdots \le \theta_{N-1}$. There are, in general, N fixed points of this transformation in $\mathbb{CP}^{N-1}$ which are $n \propto (0, \ldots, 1, \ldots, 0)$.

Note that, being the classical theory scale invariant, solutions depend only on the ratios of physical length scales, for example the ratio of the instanton size λ and of the compactification period L. The two limits, of small and large compactification periods, which are properly defined by changing L while keeping the instanton scale λ fixed, can be equivalently studied by keeping the length of the period fixed while changing λ. Hence in this paper we frequently refer to the limit $\lambda \to 0$ with $L = 1$ as the decompactification limit.

Next we parametrize the $\mathbb{CP}^{N-1}$ space by using a vector w with $N-1$ complex components w_j where $j = 1, \ldots, N-1$ defined by

$$n = \frac{1}{\sqrt{1 + |w|^2}} \begin{pmatrix} 1 \\ w_j \end{pmatrix}. \tag{2.5}$$

Strictly speaking, in this formulation, we need more patches in order to cover entirely the $\mathbb{CP}^{N-1}$ space. This can be done by using also $u_j = \frac{1}{w_j}$. The metric in the w_j coordinates is the Fubini-Study one

$$g_{\bar{i}j} = \partial_{\bar{i}} \partial_j \log(1 + |w|^2), \tag{2.6}$$

where $|w|^2 = \sum_{j=1}^{N-1} |w_j|^2$. By defining, for simplicity, $\bar{w} \cdot v = g_{\bar{i}j} \bar{w}_{\bar{i}} v_j$, the action of the sigma model can be rewritten as

$$S = \int d^2x (\partial_\mu \bar{w} \cdot \partial_\mu w). \tag{2.7}$$

It is convenient to introduce complex coordinates to parametrize the plane $z = x_1 + ix_2$, $\bar{z} = x_1 - ix_2$ and introduce corresponding complex derivatives $\partial = (\partial_{x_1} - i\partial_{x_2})/\sqrt{2}$, $\bar{\partial} = (\partial_{x_1} + i\partial_{x_2})/\sqrt{2}$. Then the action becomes

$$S = \int d^2z (\bar{\partial} w \cdot \partial \bar{w} + \partial w \cdot \bar{\partial} \bar{w}). \tag{2.8}$$

Note that (2.8) is already in a Bogomol'nyi form. For example, for holomorphic solutions $\bar{\partial} w = \partial \bar{w} = 0$ and so the first term vanishes while the second term, by using (2.6), becomes a total derivative $\partial w \cdot \bar{\partial} \bar{w} = \partial \bar{\partial} \log(1 + |w|^2)$. The action can then be calculated by using the divergence theorem in two dimensions and is given by $S = 2\pi k$, where k is the maximal degree of the rational functions w_i (assuming no overall factors).

In a toric formulation the $\mathbb{CP}^{N-1}$ space corresponds to a $N-1$ dimensional real torus fibered over a $N-1$ real dimensional simplex. An example for $\mathbb{CP}^2$ is presented in Fig. 1. The torus shrinks to a circle on the edges of the simplex and shrinks to a point on the vertices, which can be chosen to be the fixed points of Ω.

Next we consider the case of the $\mathbb{CP}^1$ sigma model on the cylinder [12]. The boundary conditions (2.4) are parametrized by one phase θ and BPS solutions are given by a single holomorphic function $w(z)$ with periodicity $w(z+1) = e^{i\theta} w(z)$. Linearity of the holomorphic solutions allows us to construct the generic one-instanton solution by summing $1/(z-m)$ poles placed on a one-dimensional lattice:

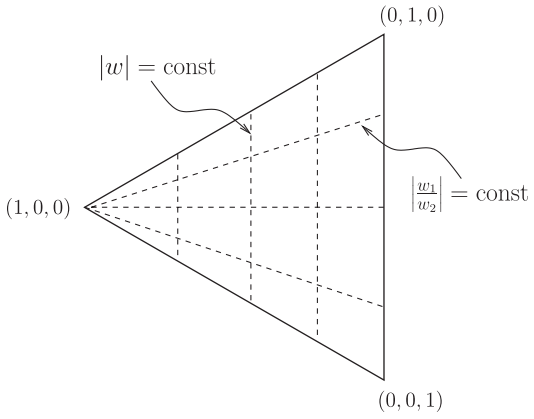

FIG. 1. Toric diagram for $\mathbb{CP}^2$.

$$w = \sum_{m=-\infty}^{\infty} \frac{\lambda e^{im\theta}}{z-m}. \tag{2.9}$$

This sum is formally divergent but it can be regularized, for example by computing its derivative first, which is convergent

$$\frac{dw}{dz} = -\sum_{m=-\infty}^{\infty} \frac{\lambda e^{im\theta}}{(z-m)^2}, \tag{2.10}$$

and then fixing the integration constant by requiring the symmetry $w(\bar{z}) = \bar{w}(z)$ which is the one respected by every single term in (2.9). For periodic and twisted boundary conditions this sum gives, respectively,

$$w = \frac{\lambda\pi}{\tan(\pi z)} \quad \text{for } \theta = 0, \text{ periodic}, \tag{2.11}$$

$$w = \frac{\lambda\pi}{\sin(\pi z)} \quad \text{for } \theta = \pi, \text{ twisted}. \tag{2.12}$$

Note that for generic θ the value of $\mathbb{CP}^1$ at $x_2 = \Im(z) \to \pm\infty$ is not the one of the single instanton poles $1/(z-m)$, which would give $n \propto (1,0)$. This happens only for the special case of $\theta = \pi$ for which we have a maximal cancellation due to the alternating phases of the poles.

Let us now study in detail the twisted solution in (2.12) and add a generic real parameter a which corresponds to the position in the x_2 coordinate

$$w = \frac{\lambda\pi}{\sin(\pi(z-ia))}. \tag{2.13}$$

We can isolate a parton inside the instanton by sending λ to infinity while keeping b_1 defined by

$$b_1 = a + \frac{\log(2\pi\lambda)}{\pi} \tag{2.14}$$

fixed. This limit gives us

$$w \to -ie^{i\pi(z-ib_1)} \quad \text{for } \lambda \to \infty, \qquad b_1 = \text{fixed}. \tag{2.15}$$

This limiting field corresponds to a kink in the x_2 direction, which interpolates between the fixed points of Ω, $n \propto (1,0)$ at $x_2 \to +\infty$ and $n \propto (0,1)$ at $x_2 \to -\infty$. In the x_1 direction it is just rotating with a phase $e^{i\pi x_1}$ so it maps the fundamental period of the cylinder into half of the $\mathbb{CP}^1$ sphere and thus it represents a parton of topological charge $1/2$. Note that, in general, this solution is parametrized only by two moduli: the position of the kink b_1 and a global phase which can also be added.

Note that we can also isolate the other parton if we define its position as

$$b_2 = a - \frac{\log(2\pi\lambda)}{\pi} \tag{2.16}$$

and then we send λ to infinity but this time keeping b_2 fixed:

$$w \to +ie^{-i\pi(z-ib_2)} \quad \text{for } \lambda \to \infty, \qquad b_2 = \text{fixed}. \tag{2.17}$$

The charge of this kink is the opposite of the previous one since it interpolates between $n \propto (0,1)$ at $x_2 \to -\infty$ and $n \propto (1,0)$ at $x_2 \to +\infty$. The phase rotation in the x_1 direction is also opposite $e^{-i\pi x_1}$ and thus the topological charge is the same as before. So as $\log\lambda \gg 1$, the soliton (2.13) splits into two partons, each carrying half of the topological charge, and located at the positions (2.14) and (2.16) [i.e. with the distance $2\log(2\pi\lambda)/\pi$ between them]. The solution becomes almost translationally invariant in the x_1 coordinate, as we can always perform a phase rotation on it.

We now show that there is another quick route to arrive at the same result. We take the conformal mapping

$$x_+ = e^{-i2\pi z/h}, \qquad h \in \mathbb{Z}, \tag{2.18}$$

which maps the cylinder with identification $z \simeq z + h$ onto the plane x_+. For the strictly periodic boundary conditions, i.e. for $\theta_i = 0$, we can choose $h = 1$ since the function is already periodic on the fundamental period of the cylinder. For generic boundary conditions, h must be taken to be the smallest integer for which the matrix Ω satisfies

$$\Omega^h = \mathbf{1}_{N,N}. \tag{2.19}$$

Note that this is possible only if θ_i are rational multiples of π. With this trick we can map the problem onto the plane x_+ by imposing strict periodicity in $\arg(x_+)$. For example for the twisted boundary in the $\mathbb{CP}^1$ case we have to choose $h = 2$ so that the cylinder contains two of the fundamental periods. For $\mathbb{CP}^2$ with twisted boundary conditions we have to choose $h = 3$; the corresponding map for this example is shown in Fig. 2.

Next we rederive the previous results for the twisted boundary conditions in the $\mathbb{CP}^1$ case from the x_+ plane perspective. The one-instanton solution (2.12) in the x_+ plane corresponds to two solitons located at $\pm e^{\pi a}$; i.e. w is given by

$$w = -2\pi\lambda e^{\pi a}\left(\frac{1}{x_+ + e^{\pi a}} + \frac{1}{x_+ - e^{\pi a}}\right). \tag{2.20}$$

In general, all solutions in the x_+ plane have the following $\mathbb{Z}_2$ symmetry:

$$w(-x_+) = -w(x_+). \tag{2.21}$$

Note that in the w plane we have a branch cut for the inverse function of (2.20). This cut goes from $w = -2i\pi\lambda$ to $w = 2i\pi\lambda$. This cut is crossed each time we move by one

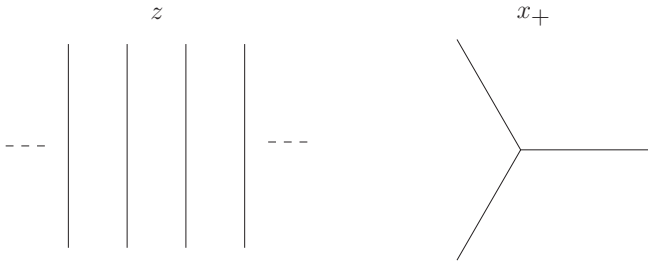

FIG. 2. Conformal map for $\mathbb{CP}^2$ with twisted boundary conditions.

fundamental period of the cylinder. The widening of the cut as $\lambda \to \infty$ is another manifestation of the fractionalization.

This can be derived from a solution on the cylinder with twisted boundary conditions and vice versa. It is also possible to have a single instanton with the $\mathbb{Z}_2$ symmetry in the x_+ plane, but only if we fix its position to be at the origin. In particular, the following one-soliton solutions in x_+ are allowed:

$$w = \frac{e^{\pi b_1}}{x_+}, \qquad w = -e^{\pi b_2} x_+. \tag{2.22}$$

They correspond, respectively, to the two partons (2.15) and (2.17). So the partons on the z cylinder correspond to one-solitons in the x_+ plane and fractionalization is just a consequence of the choice $h = 2$ for the conformal mapping (2.18).

We can use this technique to describe partons in $\mathbb{CP}^2$. The twisted boundary conditions correspond to

$$\Omega = \mathrm{diag}(1, \omega, \omega^2) \tag{2.23}$$

with $\omega = e^{i2\pi/3}$. So to go further we have to choose a conformal transformation (2.18) with $h = 3$ in order to have strict periodicity in $\arg(x_+)$. Thus we have to restrict our attentions to solutions which have the following $\mathbb{Z}_3$ symmetry:

$$\begin{pmatrix} w_1(\omega x_+) \\ w_2(\omega x_+) \end{pmatrix} = \begin{pmatrix} \omega w_1(x_+) \\ \omega^2 w_2(x_+) \end{pmatrix}. \tag{2.24}$$

Thus one-soliton solutions in the x_+ plane with this $\mathbb{Z}_3$ symmetry are given by

$$\begin{pmatrix} w_1 \\ w_2 \end{pmatrix} = \begin{pmatrix} \zeta/x_+ \\ 0 \end{pmatrix}, \qquad \begin{pmatrix} w_1 \\ w_2 \end{pmatrix} = \begin{pmatrix} 0 \\ \zeta x_+ \end{pmatrix}, \tag{2.25}$$

which are the direct generalizations of (2.22) and ζ is an arbitrary complex number. Each of these solutions in the z cylinder case corresponds to a parton with fractional charge $1/3$, and again this follows directly from the choice $h = 3$ we have made earlier. The first parton is described by a kink that interpolates from $n \propto (1, 0, 0)$ to $n \propto (0, 1, 0)$ and the second one interpolates from $n \propto (0, 1, 0)$ to $n \propto (1, 0, 0)$.

We also have another possibility, which cannot be seen in the w patch and which corresponds to n being of the form

$$n \propto \begin{pmatrix} 0 \\ 1/x_+ \\ \zeta x_+ \end{pmatrix}. \tag{2.26}$$

This expressions corresponds to a third parton which interpolates from $n \propto (0, 1, 0)$ to $n \propto (0, 0, 1)$. All these three partons together cover the perimeter of the toric diagram in Fig. 1.

We have thus seen that the conformal map (2.18) is a convenient tool to analyze solutions on $\mathbb{R} \times S^1$. In particular, it maps the infinite chain of solitons to a finite number of them related by some form of the $\mathbb{Z}_h$ symmetry. Also, the fractionalization has a simple interpretation here. There is no actual fractionalization in the x_+ plane, but there can be in the z cylinder case due to the map (2.18) when h is greater than one.

So far we have just rederived some known results [12–14], but for the nonholomorphic solutions this map will be particularly useful to perform the required computations and to derive new results.

III. NONHOLOMORPHIC SOLUTIONS AND THEIR GENERATORS

Given a generic N vector f_I its corresponding state in $\mathbb{CP}^{N-1}$ in the n formulation is

$$n_I = \frac{f_I}{|f|}. \tag{3.1}$$

Note that this choice corresponds to (2.5) in which f_I was obtained from w by multiplying it by all denominators of the components of w (and then dropping all common factors).

The P_+ operator is defined to act on f as follows:

$$(P_+ f)_I = \partial_+ f_I - \frac{f_J^\dagger \partial_+ f_J}{|f|^2} f_I. \tag{3.2}$$

Thus the P_+ operator retains only the part of $\partial_+ f_I$ which is orthogonal to f_I. Its related vector $P_+ n$ is given by

$$(P_+ n)_I = \frac{(P_+ f)_I}{|P_+ f|}. \tag{3.3}$$

It is easy to see that $P_+ n$ only changes by an irrelevant overall phase if the vector f is multiplied by an arbitrary function. As is well known [2] the P_+ operator maps a solution of the $\mathbb{CP}^{N-1}$ sigma model into another solution; that is, if n solves the Euler-Lagrange equations (2.2), then so does $P_+ n$ [2].

It is convenient to introduce a wedge product formulation. We define $f \wedge \partial_+ f$ to be

$$(f\wedge\partial_+ f)_{IJ} = f_I\partial_+ f_J - f_J\partial_+ f_I \tag{3.4}$$

and similarity for $(f\wedge\partial_+ f\wedge\partial_+^2 f)_{IJK}$. In this formulation the P_+ operator (3.2) is given by

$$(P_+ f)_I = \frac{f_J^\dagger (f\wedge\partial_+ f)_{IJ}}{|f|^2} \tag{3.5}$$

and its repeated action

$$(P_+^2 f)_I = \frac{(f\wedge\partial_+ f)^\dagger_{JK}(f\wedge\partial_+ f\wedge\partial_+^2 f)_{IJK}}{|f\wedge\partial_+ f|^2}. \tag{3.6}$$

In the $\mathbb{CP}^2$ case the wedge products simplify considerably. We can introduce a vector B and a function A defined as follows:

$$\begin{aligned}(f\wedge\partial_+ f)_{IJ} &= \frac{1}{2}\epsilon_{IJK}B_K,\\ (f\wedge\partial_+ f\wedge\partial_+^2 f)_{IJK} &= \epsilon_{IJK}A.\end{aligned} \tag{3.7}$$

With these definitions we find that, up to overall factors, which cancel in n,

$$\begin{aligned}(P_+ f)_I &\propto -\frac{\epsilon_{IJK}f_J^\dagger B_K}{|f|^2},\\ (P_+^2 f)_I &\propto -\frac{B_I^\dagger A}{|\partial_+ f|^2}.\end{aligned} \tag{3.8}$$

The expressions for the actions of the corresponding solutions are given by

$$S[n] = R_1, \qquad S[P_+ n] = R_1 + R_2, \tag{3.9}$$

where

$$R_1 = \frac{|P_+ f|^2}{|f|^2} \quad \text{and} \quad R_2 = \frac{|P_+^2 f|^2}{|P_+ f|^2}. \tag{3.10}$$

All this is true also in a general $\mathbb{CP}^{N-1}$ model. For $\mathbb{CP}^2$ we also have $S[P_+^2 n] = R_2$ and so

$$S[P_+ n] = S[n] + S[P_+^2 n]. \tag{3.11}$$

Moreover for the $\mathbb{CP}^2$ case the expressions for $R_{1,2}$ simplify further:

$$R_1 = \frac{|B|^2}{|f|^4} \quad \text{and} \quad R_2 = \frac{|A|^2|f|^2}{|B|^4}. \tag{3.12}$$

As is well known, for $\mathbb{CP}^1$ there are only holomorphic and antiholomorphic solutions. If $f = \begin{pmatrix}1\\ w\end{pmatrix}$ with w holomorphic, then

$$P_+ f \propto \begin{pmatrix}-\bar{w}\\ 1\end{pmatrix}, \tag{3.13}$$

and so the action of P_+ on k solitons creates k antisolitons and a further action of P_+ on the antisolitons produces vacuum. We can characterize a generic solution by a pair of integers (a, b), where a is the number of solitons and b the number of antisolitons. In this terminology, the chain of the operations of the P_+ operator gives

$$(k, 0) \overset{P_+}{\to} (0, k) \overset{P_+}{\to} (0, 0). \tag{3.14}$$

For $\mathbb{CP}^2$ there are in addition also non-BPS solutions. A one-soliton solution can always be treated as lying in a $\mathbb{CP}^1$ space embedded into $\mathbb{CP}^2$. So the action of the P_+ operator on such a field configuration does not produce any nontrivial non-BPS solutions. To obtain non-BPS solutions the initial configuration has to contain at least two solitons.

Consider a $\mathbb{CP}^2$ holomorphic solution describing k solitons which in the w patch is given by

$$\begin{pmatrix}w_1\\ w_2\end{pmatrix} = \sum_{\alpha=1}^{k}\begin{pmatrix}\frac{\zeta_\alpha}{x_+-\xi_\alpha}\\ \frac{\varrho_\alpha}{x_+-\xi_\alpha}\end{pmatrix}. \tag{3.15}$$

The complex numbers ζ_α, ϱ_α, ξ_α parametrize a moduli space of dimension $6k$. This is the most generic k-soliton solution with $n = (1, 0, 0)$ fixed at infinity. To compute the polynomial vector f we first find the corresponding n as defined in (2.5) and then bring all terms to a common denominator so that the final vector takes the form

$$f = \begin{pmatrix}\prod_{\alpha=1}^k (x_+ - \xi_\alpha)\\ \sum_{\alpha=1}^k \zeta_\alpha \prod_{\beta\neq\alpha}^k (x_+ - \xi_\beta)\\ \sum_{\alpha=1}^k \varrho_\alpha \prod_{\beta\neq\alpha}^k (x_+ - \xi_\beta)\end{pmatrix}. \tag{3.16}$$

The first component of f has degree k while the others have at most degree $k-1$. We know from (3.8) that $P_+^2 f \propto B^\dagger$ with B given in (3.7), so $P_+^2 f$ contains only antisolitons and their maximal number is $2k-2$. The chain of actions of the P_+ operator for $\mathbb{CP}^2$ is thus in general

$$(k, 0) \overset{P_+}{\to} (2k-2, k) \overset{P_+}{\to} (0, 2k-2). \tag{3.17}$$

Note that $2k-2$ is an upper bound on the possible number of anti-instantons in the $P_+^2 f$ solution, but for some configurations the number of antisolitons that are generated can be smaller. The simplest example is the case in which all the k solitons can be embedded into a $\mathbb{CP}^1 \subset \mathbb{CP}^2$ for which (3.14) must be true. The moduli space of k solitons in $\mathbb{CP}^2$ has dimension $6k$ while the moduli space of k solitons embedded in a generic $\mathbb{CP}^1$ has dimension $4k+2$ (the extra 2 comes from the different embeddings).

Moreover, there are other submanifolds where b, the dimension of this subspace, satisfies $0 < b < 2k-2$.

For example, if we impose the conditions

$$\sum_\alpha \zeta_\alpha = 0 \quad \text{and} \quad \sum_\alpha \varrho_\alpha = 0, \tag{3.18}$$

then we have at most $2k-3$ solitons. To have at most $2k-4$ solitons we have to impose also

$$\sum_{\alpha\neq\beta} \zeta_\alpha \xi_\beta = 0 \quad \text{and} \quad \sum_{\alpha\neq\beta} \varrho_\alpha \xi_\beta = 0 \tag{3.19}$$

and so on up to a minimum of $k-1$. So we have a sequence of nested manifolds of dimension $6k-4d$ which have at most $2k-2-d$ antisolitons in $P_+^2 f$ with $d = 0, 1, \ldots, k+1$. Note that the manifold of dimension $4k+2$ of solutions embeddable in $\mathbb{CP}^1$ is not completely contained in the previous ones, as it is clear, for example, by considering the dimensionality of the smallest manifold whose dimension is $2k-4$. The reason for this is that reducing the degree of polynomials in f is not the only way to reduce the number of instantons. This can be achieved also by arranging for all $f_{1,2,3}$ to have a common factor. Such conditions are easy to discuss in each concrete case but much harder to describe for a general configuration.

IV. EXAMPLES: EMBEDDING, CLUSTERING AND DECOMPACTIFICATION LIMITS

The conformal mapping (2.18) maps solutions of the Euler-Lagrange equations into other solutions, and this is true not only for the holomorphic or antiholomorphic solutions but also for the non-BPS ones. So all the solutions on the cylinder are mapped into the subset of solutions in the x_+ plane which satisfy a certain $\mathbb{Z}_h$ constraint. The theorems proved in [2–4] which assumed the finiteness of the total action can then be applied too and we also know that the $P_\pm$ operators generate all solutions.

To see how this works let us first take two solitons in the x_+ plane of size λ located at positions ± 1. In the w formulation they are given by

$$\begin{pmatrix} w_1 \\ w_2 \end{pmatrix} = \begin{pmatrix} \frac{c\lambda}{x_+ - 1} \\ \frac{s\lambda}{x_+ - 1} \end{pmatrix} + \begin{pmatrix} \frac{c\lambda}{x_+ + 1} \\ \frac{-s\lambda}{x_+ + 1} \end{pmatrix}, \tag{4.1}$$

where we have abbreviated $s = \sin(\alpha)$, $c = \cos(\alpha)$. Each soliton is separately embedded in a $\mathbb{CP}^1 \subset \mathbb{CP}^2$, but the configuration is not the most general two-soliton solution of $\mathbb{CP}^2$. The angle α parametrizes the different orientations of these embeddings. In particular, the whole solution can be embedded in a unique $\mathbb{CP}^1$ only for the special cases $\alpha = 0,\ \pi/2$. These solutions describe a $\mathbb{Z}_2$ symmetric configuration corresponding to the boundary condition

$$\Omega = \mathrm{diag}(1, -1, 1), \tag{4.2}$$

which can be obtained via the conformal mapping (2.18) with $h = 2$. This case is simpler than the one with the twisted boundary conditions and realizes all the phenomena that are of interest to us. The vector f, with polynomial components, corresponding to (4.1) is

$$f = \begin{pmatrix} x_+^2 - 1 \\ 2c\lambda x_+ \\ 2s\lambda \end{pmatrix}. \tag{4.3}$$

Computing B and A, defined in (3.7), we get

$$B = \begin{pmatrix} -4sc\lambda^2 \\ 4s\lambda x_+ \\ -2c\lambda(x_+^2 + 1) \end{pmatrix} \quad \text{and} \quad A = 4c\lambda(x_+^2 - 1). \tag{4.4}$$

The two antisolitons, at the end of the chain (3.17), by using (3.8), are given by

$$P_+^2 f \propto \begin{pmatrix} 2s\lambda \\ -2sx_-/c \\ x_-^2 + 1 \end{pmatrix} = \begin{pmatrix} 2\tilde{s}\,\tilde{\lambda} \\ 2\tilde{c}\,\tilde{\lambda}\, x_- \\ x_-^2 + 1 \end{pmatrix}. \tag{4.5}$$

The last equality in (4.5) involves rewriting the previous expression in a form similar to (4.3) but in a different w patch and with a different angle $\tilde{\alpha}$ and of different size $\tilde{\lambda}$. We again abbreviated $\tilde{s} = \sin(\tilde{\alpha})$ and $\tilde{c} = \cos(\tilde{\alpha})$. The relation between the new angle and size and the old ones is given by

$$\tilde{\alpha} = -\arctan(\lambda c), \qquad \tilde{\lambda} = -t\sqrt{1 + c^2\lambda^2}. \tag{4.6}$$

So the two antisolitons, at the end of the chain, are always located at fixed positions $\pm i$ and have their relative orientation and size determined by $\tilde{\alpha}$, $\tilde{\lambda}$.

The first interesting limit to explore is when the relative orientation of the two solitons goes to zero. This limit corresponds to the case (3.14) in which the whole holomorphic solution can be embedded into a unique $\mathbb{CP}^1$ and thus no antisolitons are created. We know that this is the case when α is strictly zero but we want to see how, when the limit is taken, the two solitons disappear. Taking the limit corresponds to letting

$$\begin{matrix} \alpha \to 0 \\ \lambda \text{ fixed} \end{matrix} \quad \Rightarrow \quad \begin{matrix} \tilde{\alpha} \to -\arctan(\lambda) \\ \tilde{\lambda} \to 0. \end{matrix} \tag{4.7}$$

Note that as $\tilde{\lambda} \to 0$ the two solitons, while remaining at fixed positions $\pm i$, become singular (and disappear as "delta" functions). So the limit is not continuous from the point of view of the action

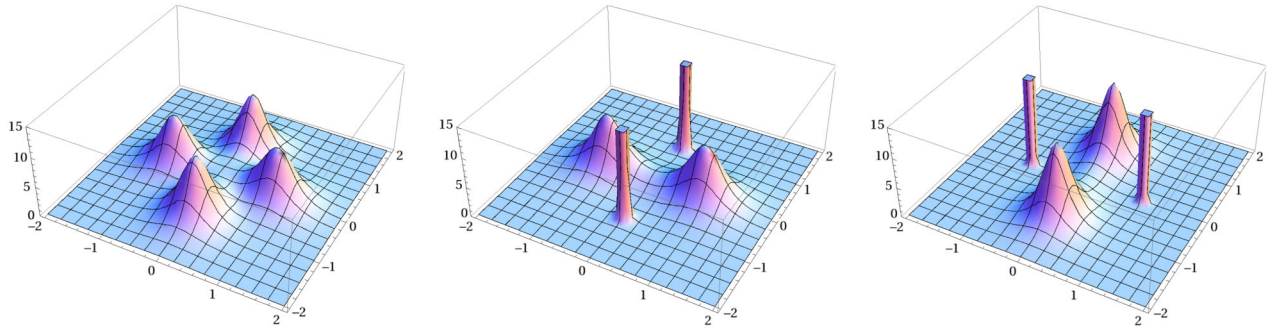

FIG. 3 (color online). Action density for $P_+ f$ with f given by the two-soliton example (4.3). $P_+ f$ is a mixture of two anti-solitons located at $x_+ = \pm 1$ and of two solitons located at $x_+ = \pm i$. The three plots correspond, respectively, to $(\alpha, \lambda) = (0.4, 0.5), (0.01, 0.5), (0.4, 0.005)$. The second plot corresponds to the α small case, thus very close to the embedding limit (4.7). The third one corresponds to the λ small case thus very close to the clustering limit (4.10).

$$4\pi = \lim_{\alpha \to 0} S[P_+^2 n(\alpha, \lambda)] \neq S[P_+^2 n(0, \lambda)] = 0. \tag{4.8}$$

The other embedding limit corresponds to $\alpha \to \pi/2$. This time, the two antisolitons disappear by becoming infinitely wide:

$$\begin{matrix} \alpha \to \pi/2 \\ \lambda \text{ fixed} \end{matrix} \quad \Rightarrow \quad \begin{matrix} \tilde{\alpha} \to 0 \\ \tilde{\lambda} \to \infty. \end{matrix} \tag{4.9}$$

Another interesting limit is that of the clustering, which corresponds to sending the distance between the two solitons to infinity while keeping their sizes and their relative angle fixed. By conformal invariance the clustering limit is equivalent to the limit $\lambda \to 0$ while keeping the distance fixed, and thus we can use the solutions of the form (4.1). This limit, on the antisolitons $P_+^2 f$, has the following effect:

$$\begin{matrix} \alpha \text{ fixed} \\ \lambda \to 0 \end{matrix} \quad \Rightarrow \quad \begin{matrix} \tilde{\alpha} \to 0 \\ \tilde{\lambda} \to -t, \end{matrix} \tag{4.10}$$

where t is some number. Note that the antisolitons remain of the fixed size in this limit. Note also that this observation demonstrates that the action of the operator P_+ is highly nonlocal and, in particular, the states it produces may not obey the clustering property. The two original solitons, after computing P_+, have an effect on each other which does not decrease or disappear as their distance is sent to infinity.

The above mentioned analysis has been done on the final step of the chain, that is, on $P_+^2 f$. The intermediate step $P_+ f$ is, in general, a mixture of the two initial and the two final solitons. So we expect the two limits (4.7) and (4.10) to produce the same result. Some examples of $S[P_+ n]$ are given in Fig. 3 for different values of α and λ. The tools described in Sec. III allow us to confirm this also analytically. Computing R_1 and R_2 defined in (3.12) for the solution (4.3) gives us

$$\begin{aligned} R_1 &= \frac{4\lambda^2(4s^2c^2\lambda^2 + 4s^2|x_+|^2 + c^2|x_+^2 + 1|^2)}{(4s^2\lambda^2 + 4c^2\lambda^2|x_+|^2 + |x_+^2 - 1|^2)^2}, \\ R_2 &= \frac{4c^2s^2\lambda^4(|x_+^2 - 1|^2 + 4c^2\lambda^2|x_+|^2 + s^2\lambda^2)}{(4s^2c^2\lambda^4 + 4s^2\lambda^2|x_+|^2 + c^2\lambda^2|x_+^2 + 1|^2)^2}. \end{aligned} \tag{4.11}$$

The action $S[P_+ n]$ is the sum of these two terms, and thus a sum of the action of the initial solution R_1 and of the final one R_2. For example, in the clustering limit $\lambda \to 0$, we have

$$\begin{aligned} R_1 &\sim \frac{4\lambda^2(4s^2|x_+|^2 + c^2|x_+^2 + 1|^2)}{(4s^2\lambda^2 + 4c^2\lambda^2|x_+|^2 + |x_+^2 - 1|^2)^2}, \\ R_2 &\to \frac{4c^2s^2|x_+^2 - 1|^2}{(4s^2|x_+|^2 + c^2|x_+^2 + 1|^2)^2}. \end{aligned} \tag{4.12}$$

The first term R_1 corresponds to the original solitons located at ± 1 shrinking to zero while the second term describes the other two solitons located at $\pm i$ which remain of fixed size and which do not disappear.

Next we move to the twisted boundary conditions (2.23). A one-soliton solution in the z cylinder corresponds in the x_+ plane to the following three-solitons with $\mathbb{Z}_3$ symmetry:

$$\begin{pmatrix} w_1 \\ w_2 \end{pmatrix} = \begin{pmatrix} \frac{c\lambda}{x_+ - 1} \\ \frac{s\lambda}{x_+ - 1} \end{pmatrix} + \begin{pmatrix} \frac{\omega^2 c\lambda}{x_+ - \omega} \\ \frac{\omega s\lambda}{x_+ - \omega} \end{pmatrix} + \begin{pmatrix} \frac{\omega c\lambda}{x_+ - \omega^2} \\ \frac{\omega^2 s\lambda}{x_+ - \omega^2} \end{pmatrix}, \tag{4.13}$$

where α, as before, is an angle parametrizing the $\mathbb{CP}^1$ of each soliton embedded into $\mathbb{CP}^2$. The polynomial vector f and $P_+^2 f$ for this solution are given by

$$f = \begin{pmatrix} x_+^3 - 1 \\ 3c\lambda x_+ \\ 3s\lambda \end{pmatrix} \quad \Rightarrow \quad P_+^2 f \propto \begin{pmatrix} 3\lambda s \\ -3x_-^2 t \\ 1 + 2x_-^3 \end{pmatrix}. \tag{4.14}$$

To interpret this result we need to decompose $P_+^2 f$ into its antisoliton components. For this we need to use a different w patch in which

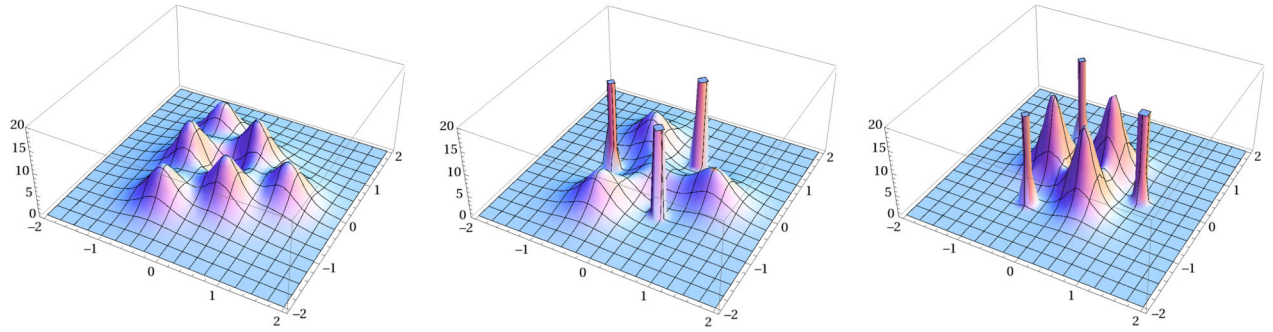

FIG. 4 (color online). Action density for P_+f for f given by the three-soliton example in (4.14). P_+f is a mixture of three antisolitons located at 1, ω, ω^2 and three solitons located at ρ, $\rho\omega$, $\rho\omega^2$. The three plots correspond, respectively, to $(\alpha,\lambda)=(0.8,0.5),(0.015,0.5),(0.8,0.01)$. The second plot corresponds to the α small case; the third one to the λ small case.

$$n=\frac{1}{\sqrt{1+|\tilde{w}|^2}}\begin{pmatrix}\tilde{w}_1\\ \tilde{w}_2\\ 1\end{pmatrix}, \tag{4.15}$$

as then $P_+^2 f$ can be decomposed into the following three antisolitons:

$$\begin{pmatrix}\tilde{w}_1\\ \tilde{w}_2\end{pmatrix}=\begin{pmatrix}\frac{\omega^2\tilde{c}\,\tilde{\lambda}}{x_--\rho}\\ \frac{\tilde{s}\,\tilde{\lambda}}{x_--\rho}\end{pmatrix}+\begin{pmatrix}\frac{\tilde{c}\,\tilde{\lambda}}{x_--\omega\rho}\\ \frac{\tilde{s}\,\tilde{\lambda}}{x_--\omega\rho}\end{pmatrix}+\begin{pmatrix}\frac{\omega\tilde{c}\,\tilde{\lambda}}{x_--\omega^2\rho}\\ \frac{\tilde{s}\,\tilde{\lambda}}{x_--\omega^2\rho}\end{pmatrix}, \tag{4.16}$$

where $\rho=\omega^{1/2}/2^{1/3}$, so that

$$P_+^2 f\propto\begin{pmatrix}3\tilde{\lambda}\,\tilde{c}\,/|\rho|\\ 6x_-^2\tilde{\lambda}\,\tilde{s}\\ 1+2x_-^3\end{pmatrix}. \tag{4.17}$$

The positions of the antisolitons are fixed and the new angle $\tilde{\alpha}$ and size $\tilde{\lambda}$ are given by

$$\tilde{\alpha}=-\arctan\left(\frac{|\rho|^2}{\lambda c}\right),\qquad \tilde{\lambda}=\frac{t}{2}\sqrt{1+\frac{\lambda^2c^2}{|\rho|^4}}, \tag{4.18}$$

and we see that $\tilde{\lambda}\to 0$ as $\alpha\to 0$ and $\tilde{\lambda}\to t/2$ as $\lambda\to 0$. Note that the applications of the P_+ operator generates the following chain:

$$(3,0)\overset{P_+}{\to}(3,3)\overset{P_+}{\to}(0,3) \tag{4.19}$$

for which the soliton numbers are smaller than in (3.17) since (4.13) satisfy the constraint (3.18). The intermediate configuration P_+f is a mixture containing six solitons in total. The embedding limit ($\alpha\to 0$ with λ fixed) and the clustering limit ($\lambda\to 0$ with α fixed) have the same features as in the previous example; some examples are shown in Fig. 4. When $\alpha\to 0,\ \pi/2$ the antisolitons disappear by becoming very peaked or very spread out. In the clustering limit $\lambda\to 0$ the antisolitons remain of fixed size.

Dabrowski and Dunne in [6] considered some fractionalized non-BPS solutions on $\mathbb{R}\times S^1$, and the simplest example is given by P_+ acting on two partons with different orientations inside $\mathbb{CP}^2$. In the x_+ plan this corresponds to the solution

$$\begin{pmatrix}w_1\\ w_2\end{pmatrix}=\begin{pmatrix}\frac{\zeta}{x_+}\\ \frac{\xi}{x_+^2}\end{pmatrix}, \tag{4.20}$$

which is the most general two-instanton solution which satisfies the $\mathbb{Z}_3$ constraint (4.16) and has $n\propto(1,0,0)$ at infinity. For $\zeta=0$ we have two coincident axial symmetric solitons embedded in the same $\mathbb{CP}^1$ and for $\zeta\neq 0$ they have different orientations. We can then use the scale invariance to fix, for example, $\xi=1$ and this fixes the center of mass of the two partons to be, in the cylinder coordinates, at $\Im(z)=0$. The other parameter ζ represents the distance, which is $d=2\log|\zeta|/\pi$ for large $|\zeta|$, and the relative phase between the two partons. Following the same procedure as in the previous examples, we find f and $P_+^2 f$ to be given by

$$f=\begin{pmatrix}x_+^2\\ \zeta x_+\\ \xi\end{pmatrix}\quad\Rightarrow\quad P_+^2 f\propto\begin{pmatrix}\xi^*\\ -2\xi^* x_-/\zeta^*\\ x_-^2\end{pmatrix}, \tag{4.21}$$

which thus tells us that at the end of the chain we have two antisolitons. The P_+n is thus a (2,2) soliton solution which in the z cylinder corresponds to four total partons. The $P_+^2 f$ is very similar to f so it can be interpreted in the same way but in a different patch and with

$$\tilde{\xi}=\xi^*,\qquad \tilde{\zeta}=-\frac{2\xi^*}{\zeta^*}. \tag{4.22}$$

Note that as $\zeta\to 0$ we have $\tilde{\zeta}\to\infty$ so in the embedding limit the two antisolitons disappear by going to infinite distance in $\Im(z)$.

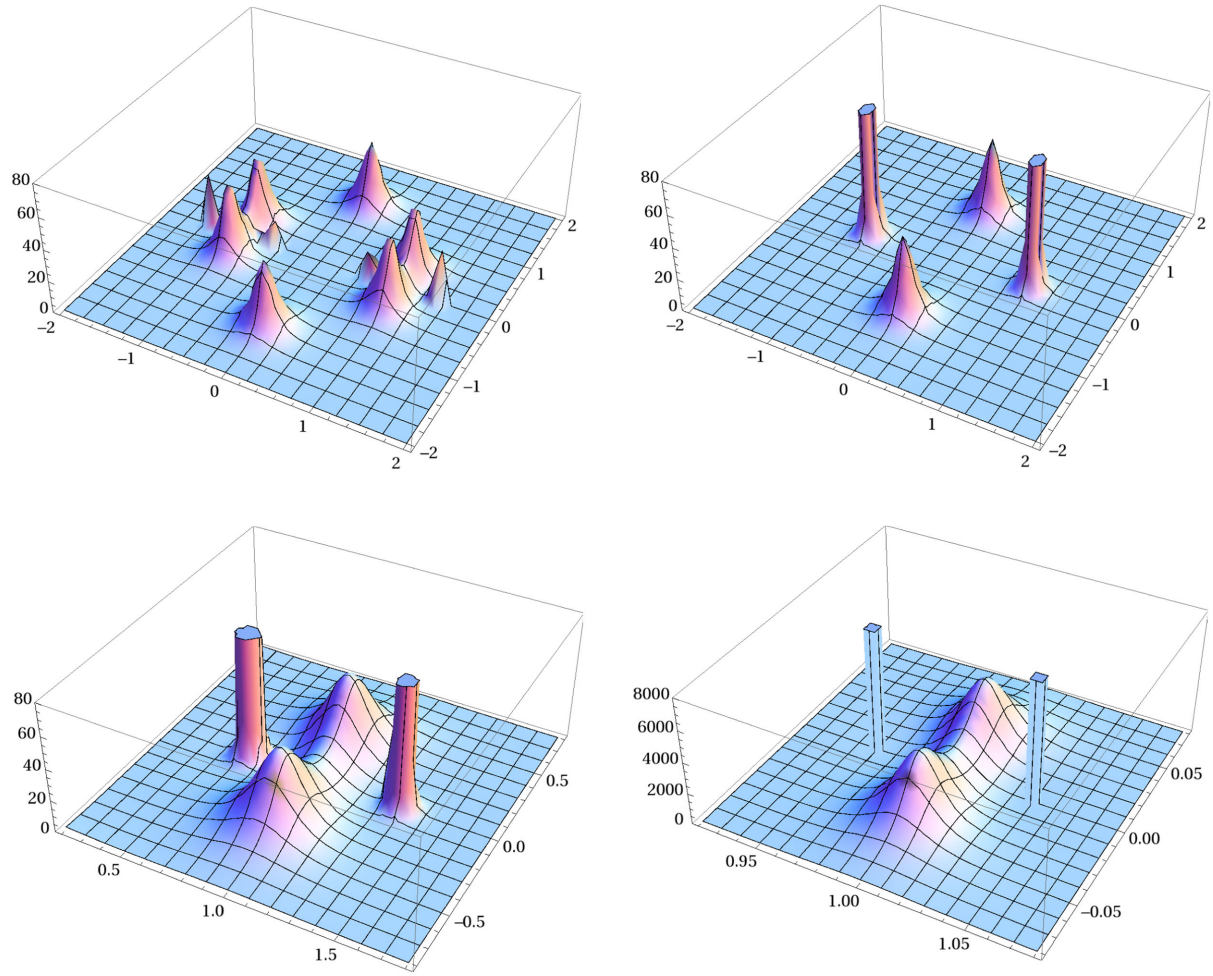

FIG. 5 (color online). The first line is the action density for $P_+ f$ of the $\mathbb{Z}_2$ symmetric configuration with four antisolitons plus six solitons (4.23) for the values $(\alpha, \lambda) = (0.2, 0.25), (0.2, 0.025)$ and $\epsilon = 1.6\lambda$. The second line is obtained by zooming into the right-hand cluster for the same values of (α, λ).

Finally we consider a four-soliton configuration. This case will allow us to demonstrate an even more severe pathology of the clustering decomposition. This time we consider four solitons with the $\mathbb{Z}_2$ symmetry (4.2):

$$\begin{pmatrix} w_1 \\ w_2 \end{pmatrix} = \begin{pmatrix} \frac{c\lambda}{x_+ - a} \\ \frac{s\lambda}{x_+ - a} \end{pmatrix} + \begin{pmatrix} \frac{c\lambda}{x_+ - b} \\ \frac{s\lambda}{x_+ - b} \end{pmatrix} + \begin{pmatrix} \frac{c\lambda}{x_+ + a} \\ \frac{-s\lambda}{x_+ + a} \end{pmatrix} + \begin{pmatrix} \frac{c\lambda}{x_+ + b} \\ \frac{-s\lambda}{x_+ + b} \end{pmatrix}. \tag{4.23}$$

This configuration consists of two solitons located at a and b and embedded in the same $\mathbb{CP}^1$ together with their $\mathbb{Z}_2$ symmetric partners located at $-a$ and $-b$. So all together we have two clusters each composed of two solitons which are separately embeddable into $\mathbb{CP}^1$. The relative angle α, as before, parametrizes the relative embedding of the two clusters. The polynomial vector f is now

$$f = \begin{pmatrix} (x_+^2 - a^2)(x_+^2 - b^2) \\ 2c\lambda x_+ (2x_+^2 - a^2 - b^2) \\ 2s\lambda(a + b)(x_+^2 - ab) \end{pmatrix}. \tag{4.24}$$

To study the clustering limit we consider

$$a = 1 + i\epsilon \quad \text{and} \quad b = 1 - i\epsilon,$$
$$\lambda, \epsilon \to 0 \quad \text{keeping } \frac{\lambda}{\epsilon}, \quad \alpha = \text{fixed}. \tag{4.25}$$

This is equivalent to sending the two clusters to an infinite distance from each other. In this limit two of the antisolitons remain at a fixed position and have a finite limiting size as before (see first line of Fig. 5). To detect the other four antisolitons we have to zoom into the individual clusters (see second line of Fig. 5). In this case we follow one cluster by zooming the lengths so that they do not change as $\lambda \to 0$. The other four antisolitons are

individually clustering with the four solitons and then follow them to the same positions, but shrinking to zero size (becoming δ functions).

The discontinuities we have found are intrinsic properties of the non-BPS solutions and not only of the P_+ operator. To see this very clearly let us take a generalized version of (4.23) given by

$$\begin{pmatrix} w_1 \\ w_2 \end{pmatrix} = \begin{pmatrix} \frac{e^{i\phi}\cos(\alpha+\beta)\lambda}{x_+-a} \\ \frac{e^{-i\phi}\sin(\alpha+\beta)\lambda}{x_+-a} \end{pmatrix} + \begin{pmatrix} \frac{e^{i\phi}\cos(\alpha-\beta)\lambda}{x_+-b} \\ \frac{e^{-i\phi}\sin(\alpha-\beta)\lambda}{x_+-b} \end{pmatrix} + \begin{pmatrix} \frac{e^{i\phi}\cos(\alpha+\beta)\lambda}{x_++a} \\ \frac{-e^{-i\phi}\sin(\alpha+\beta)\lambda}{x_++a} \end{pmatrix} + \begin{pmatrix} \frac{e^{i\phi}\cos(\alpha-\beta)\lambda}{x_++b} \\ \frac{-e^{-i\phi}\sin(\alpha-\beta)\lambda}{x_++b} \end{pmatrix}. \quad (4.26)$$

The angles α and ϕ describes the relative orientation between the two clusters inside $\mathbb{CP}^2$, while the angle β describes the relative orientation between the two solitons within each cluster. We want to consider the clustering limit of P_+f by using (4.25) and keeping β fixed and, in general, being different from 0, $\pi/2$. In this limit the two clusters flow separately to two non-BPS solutions of $2+2$ total solitons each. By computing explicitly $P_+^2 f$ we can see that there are now six antisolitons, in general, and that the number of very thin ones (corresponding to δ functions) can, at most, be reduced to five by the choice of the relative orientation $\alpha = \pi/2$; thus this number can never drop to four which would be required to have good clustering properties.

Having studied the clustering properties for a number of examples of non-BPS solutions, we can now turn our attention to the same problem for the $\mathbb{CP}^{N-1}$ model on $\mathbb{R}\times S^1$ (with twisted boundary conditions) and study the correspondence between the solutions at large and small compactification radii in this model. We have already said that, by conformal mapping, the planar limit (or decompactification limit) of this model is equivalent to what we called before the clustering limit in the x_+ plane. As the BPS solutions are continuously connected, the dimension of their moduli space and of the action remain the same during the change of the compactification radius. A number of discontinuities, however, arise for the non-BPS solutions. The first class of them is exemplified by the clustering limit of the examples (4.1) and (4.13). These solutions, when pulled back to the z cylinder, do not flow to a localized solution in $\mathbb{R}^2$. There is always a residual contribution on the opposite side of the cylinder coordinates, even when its radius is sent to infinity. This shows that the set of solutions on the cylinder is slightly "larger" than the set of solutions in the plane; there is no one-to-one correspondence between the two formulations.

The example (4.26) demonstrates another kind of discontinuity. In this case, after the mapping to the z cylinder, we have a local non-BPS solution which can never be recovered smoothly from a non-BPS solution on the cylinder. So not only there are more solutions on $\mathbb{R}\times S^1$ than on $\mathbb{R}^2$, but also there are not, in general, continuous mappings between them.

V. CONCLUSION

In this paper we have discussed and compared the solutions of the $\mathbb{CP}^{N-1}$ nonlinear sigma model on the plane and on the cylinder. We used a conformal mapping technique to rederive some results concerning the holomorphic solutions on $\mathbb{R}\times S^1$ with twisted boundary conditions. We then discussed some aspects of the generators of nonholomorphic solutions and showed some discontinuities in these equations that arise in various limits. In particular, the examples we studied in Sec. IV show some pathological features of the clustering limit for non-BPS solutions due to the nonlocality of the P_+ operator. Thus if we take k solitons, divide them into two groups or clusters $k_1+k_2=k$ and send these two clusters to infinite distances while keeping fixed their internal structure, the naive expectation would be that their mutual influence vanishes in this limit. However, for the P_+ operator this is not true; in other words, P_+ of the k solitons is not equal to P_+ of the two individual clusters, even when we send these clusters to infinite distances.

This also implies that the decompactification limit of $\mathbb{R}\times S^1$ for the non-BPS solitons is not in general continuous for generic non-BPS solutions. So the set of solutions of the $\mathbb{CP}^{N-1}$ sigma model on the plane $\mathbb{R}^2$ cannot be continuously related to the set of solutions on the cylinder $\mathbb{R}\times S^1$. Any extrapolation of results from small to big radii for the non-BPS solutions must carefully address these issues.

Of course, since these discontinuities arise only in the non-BPS sector, they would not affect the one-soliton sector in any $\mathbb{CP}^{N-1}$ model, which is always BPS. So for example it would not affect the results discussed in [9–11] which concern the first contribution to the transseries due to one single parton. But to be able to use the compactification method to compute the whole series, or to even prove the existence of a well defined series, a more detailed analysis of these discontinuities for non-BPS solutions would be required. Note that here we are using the concept of continuity in the strong sense with the natural topology being provided by the action. Trying to define convergence in a weaker sense, if properly formulated, may help in further developments. This problem is currently under active consideration.

ACKNOWLEDGMENTS

This work is partially funded by EPSRC Grant No. EP/K003453/1.

[1] A. D'Adda, M. Luscher, and P. Di Vecchia, Nucl. Phys. **B146**, 63 (1978).
[2] A. M. Din and W. J. Zakrzewski, Nucl. Phys. **B174**, 397 (1980).
[3] A. M. Din and W. J. Zakrzewski, Phys. Lett. **95B**, 426 (1980).
[4] A. M. Din and W. J. Zakrzewski, Nucl. Phys. **B182**, 151 (1981).
[5] W. J. Zakrzewski, *Low Dimensional Sigma Models* (Hilger, London, 1989).
[6] R. Dabrowski and G. V. Dunne, Phys. Rev. D **88**, 025020 (2013).
[7] A. Cherman, D. Dorigoni, G. V. Dunne, and M. Unsal, Phys. Rev. Lett. **112**, 021601 (2014).
[8] G. Basar, G. V. Dunne, and M. Unsal, J. High Energy Phys. 10 (2013) 041.
[9] P. C. Argyres and M. Unsal, J. High Energy Phys. 08 (2012) 063.
[10] G. V. Dunne and M. Unsal, J. High Energy Phys. 11 (2012) 170.
[11] G. V. Dunne and M. Unsal, Phys. Rev. D **87**, 025015 (2013).
[12] F. Bruckmann, Phys. Rev. Lett. **100**, 051602 (2008).
[13] W. Brendel, F. Bruckmann, L. Janssen, A. Wipf, and C. Wozar, Phys. Lett. B **676**, 116 (2009).
[14] D. Harland, J. Math. Phys. (N. Y.) **50**, 122902 (2009).